Electronic supplementary information

Heterostructure enhanced sodium storage performance for SnS_2 in hierarchical SnS_2/Co_3S_4 nanosheet array composite

Lele Cheng, Yingmeng Zhang, Panpan Chu, Suhang Wang, Yongliang Li, Xiangzhong Ren, Peixin Zhang and Lingna Sun*

College of Chemistry and Environmental Engineering, Shenzhen University, Shenzhen, Guangdong 518060, P.R. China. Tel/Fax: +86-755-26538657, E-mail: lindasun1999@126.com; sunln@szu.edu.cn

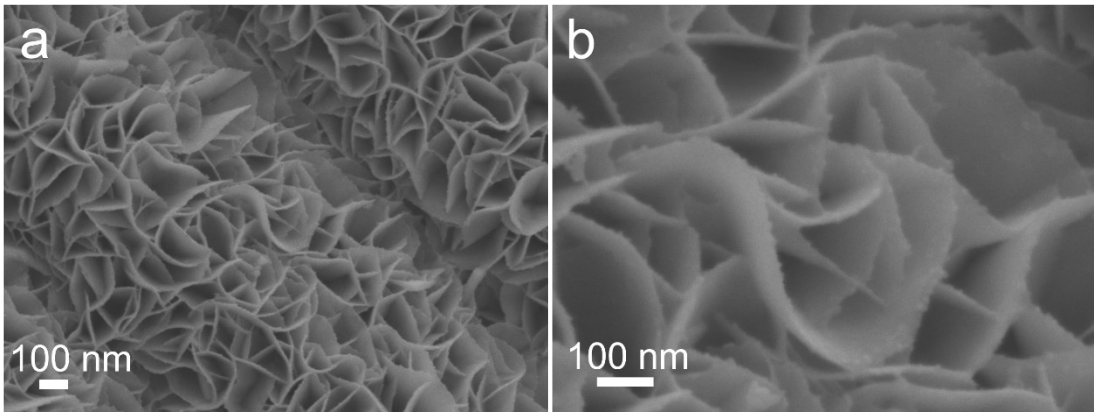

Fig. S1. The morphology characterization of the SnS_2@CC composite: Low magnification (a); high magnification SEM image (b).

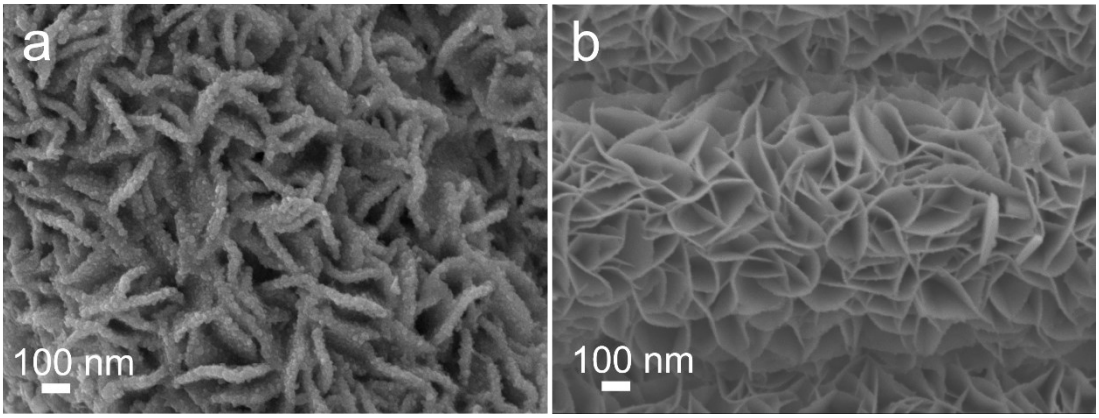

Fig. S2 The morphology characterization of the SnS_2/Co_3S_4@CC (a) and the SnS_2@CC (b) composite: SEM images magnification was 3000 times.

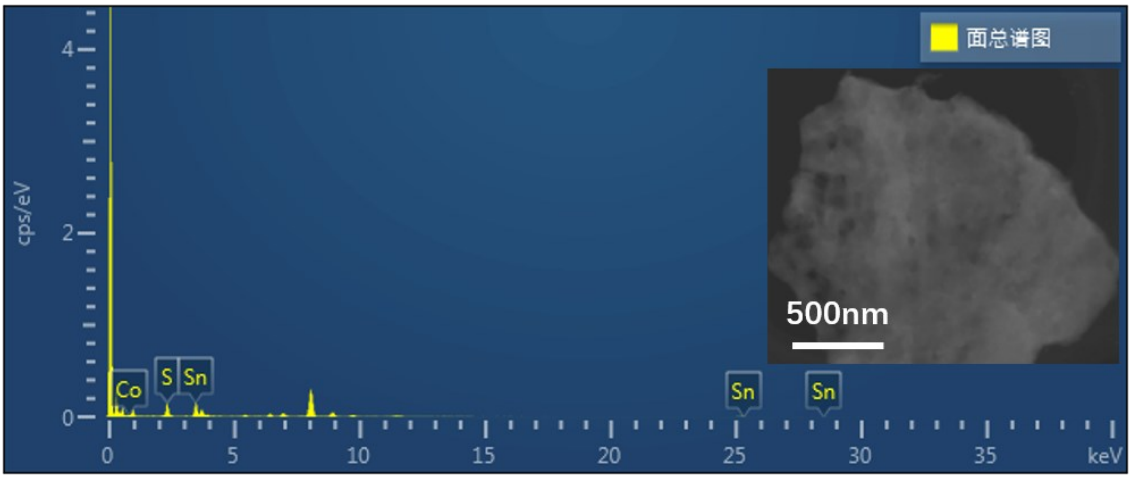

Fig. S3 The energy dispersive X-ray spectrum of the SnS_2/Co_3S_4 heterostructure nanosheets.

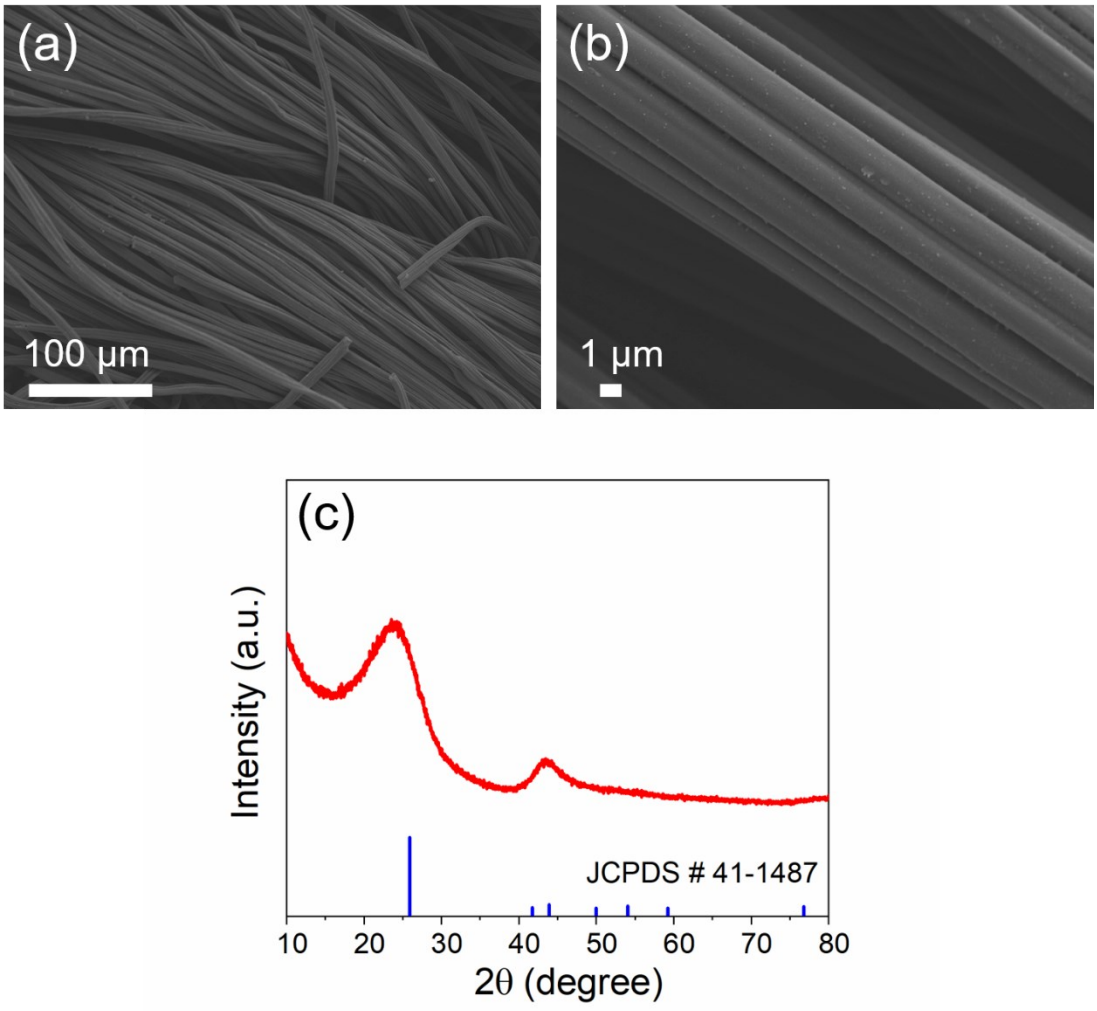

Fig. S4 The Co_3S_4 samples grown on carbon fabric by oil bath method: low magnification (a); high magnification SEM image (b); the XRD pattern(a).

By using the oil bath method, controlling the same experimental conditions, try to grow Co_3S_4 nanoparticles on the treated carbon cloth fibers. It was observed that the carbon cloth fiber bundle was very smooth, and no other special shapes were found. In the XRD test, except for indicating that under the same experimental conditions, Co_3S_4 nanoparticles could not grow on carbon cloth fibers through an oil bath. Apart from the relatively flat carbon peak, no other characteristic diffraction peaks were found.

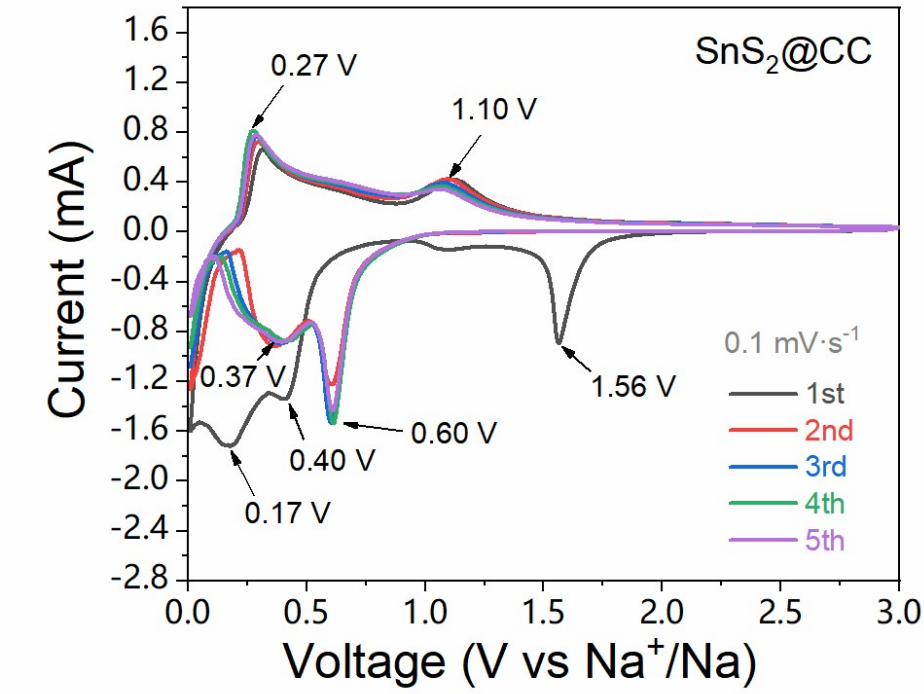

Fig. S5 The initial five CV curves of the SnS_2@CC electrode at a scan rate of 0.1 $mV \cdot s^{-1}$ between 0.01 and 3.0 V.

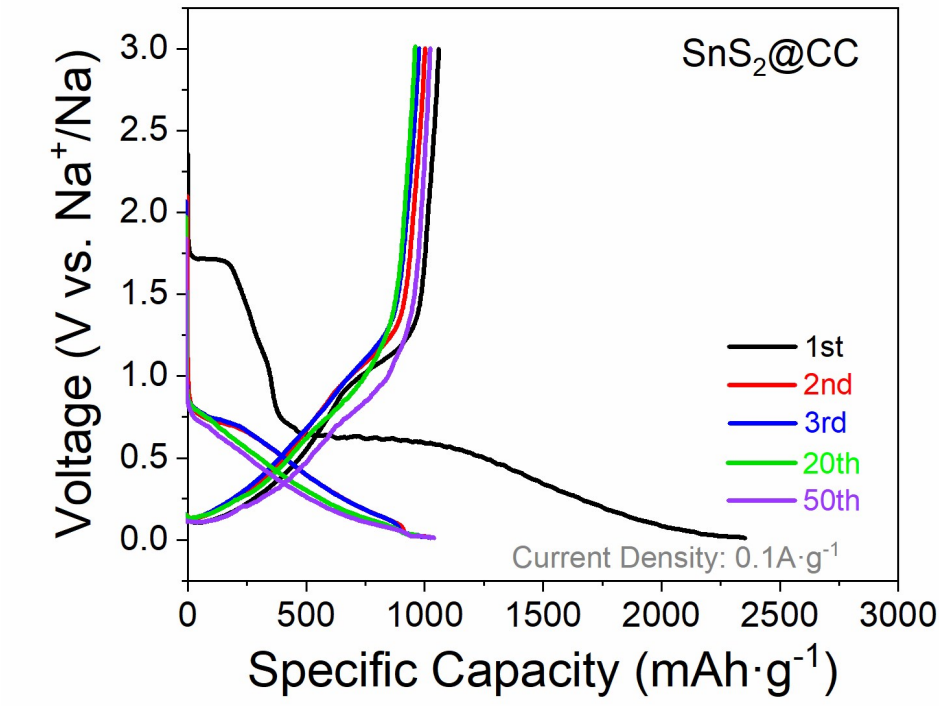

Fig. S6 Galvanostatic charge/discharge profiles during the first, second, third, 20th and 50th cycles of the SnS_2@CC electrode at current density of 0.1 $A \cdot g^{-1}$.

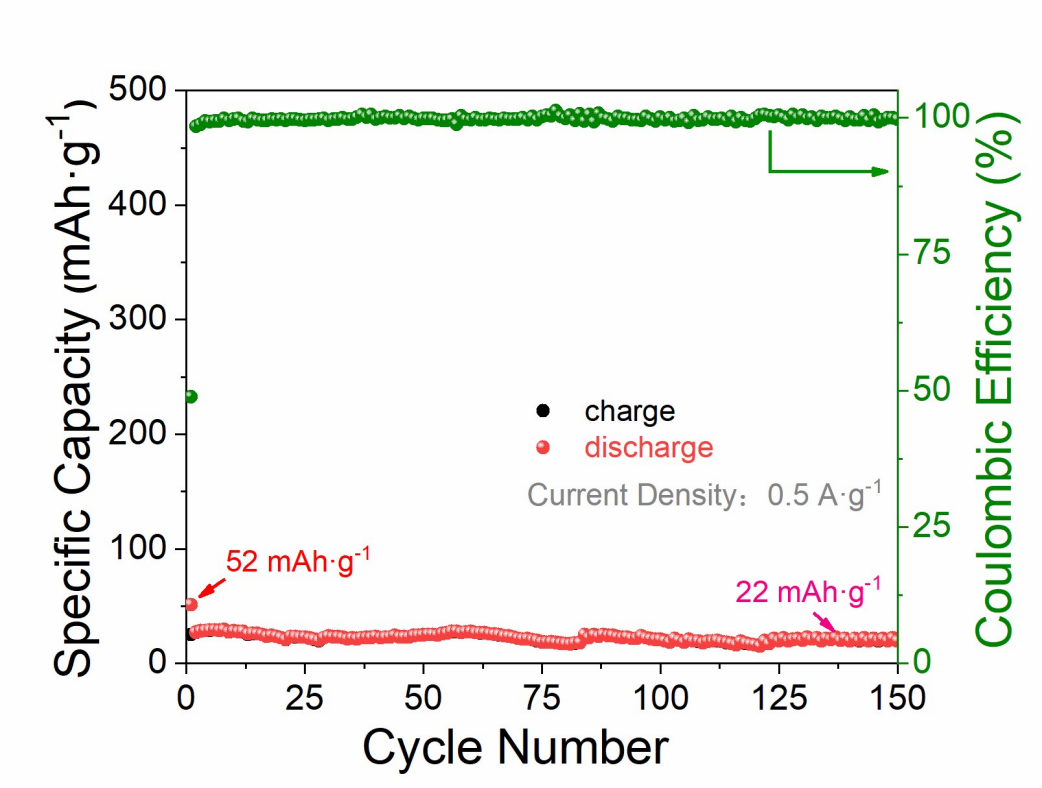

Fig. S7 Cycling performance at 0.5 $A \cdot g^{-1}$ for the pure carbon cloth fibers.

Table S1. Comparison of the electrochemical performance of SnS_2/Co_3S_4@CC anodes with other Sn-based sulfides used in SIBs in recent papers.

Materials description	Cycling data	Rate capability	Reference
SnS on graphene foam	1010/200th/0.1C	410/30C	1
SnS_2/rGO	627/100th/0.2C		2
SnS nanorods	370/30th/0.125C	300/1C	3
SnS/SnO_2	409/500th/0.81C	430/2.43C	4
SnS_2/graphene	670/60th/0.02C	670/60th/0.02C	5
SnS_2/N-graphene	450/100th/0.2C	148/10C	6
SnS_2–rGO composite	628/100th/0.2C	544/2C	7
SnS_2/CC	1039.9/130th/0.2 Ag^{-1}	673.4/400th/2 Ag^{-1}	8
SnS_2/Co_3S_4-rGO	1141.8/50th/0.1 Ag^{-1}	845.7/100th/0.5 Ag^{-1}	9
ZnS/SnS_2@NSC	537.8/120th/1 Ag^{-1}	456.2/100th/5 Ag^{-1}	10
SnS_2/Co_3S_4@CC	1259.5/100th/0.1 Ag^{-1}	637.2/760th/2 Ag^{-1}	this work

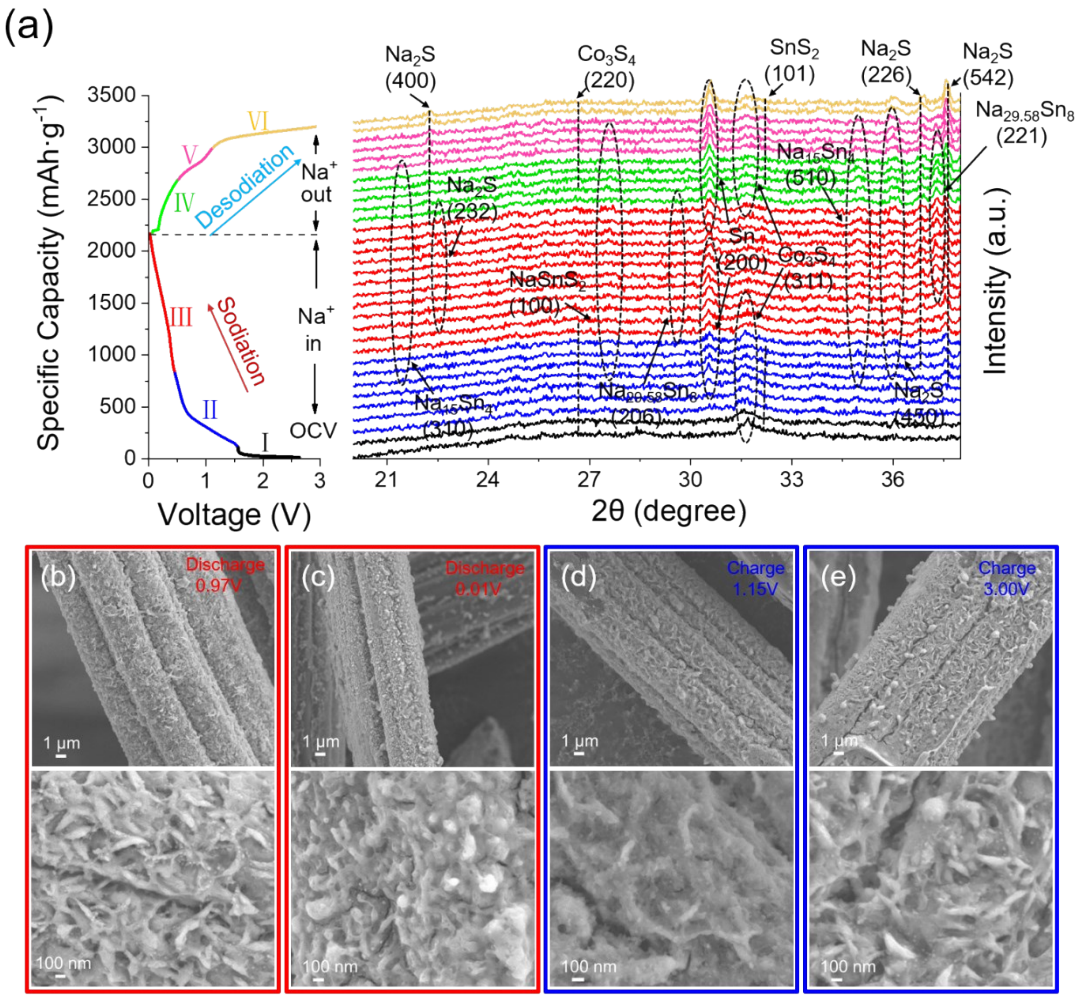

Fig. S8 Selective in-situ XRD patterns at different discharge/charge stages obtained at current density of 0.1 A g^{-1} within a potential window from 0.01 to 3.0 V (a); Ex situ FESEM images of SnS_2/Co_3S_4@CC electrodes at sodiated states of 0.97 V (b1, b2) and 0.01 V (c1, c2) and desodiated states of 1.15 V (d1, d2) and 3.00 V (e1, e2).

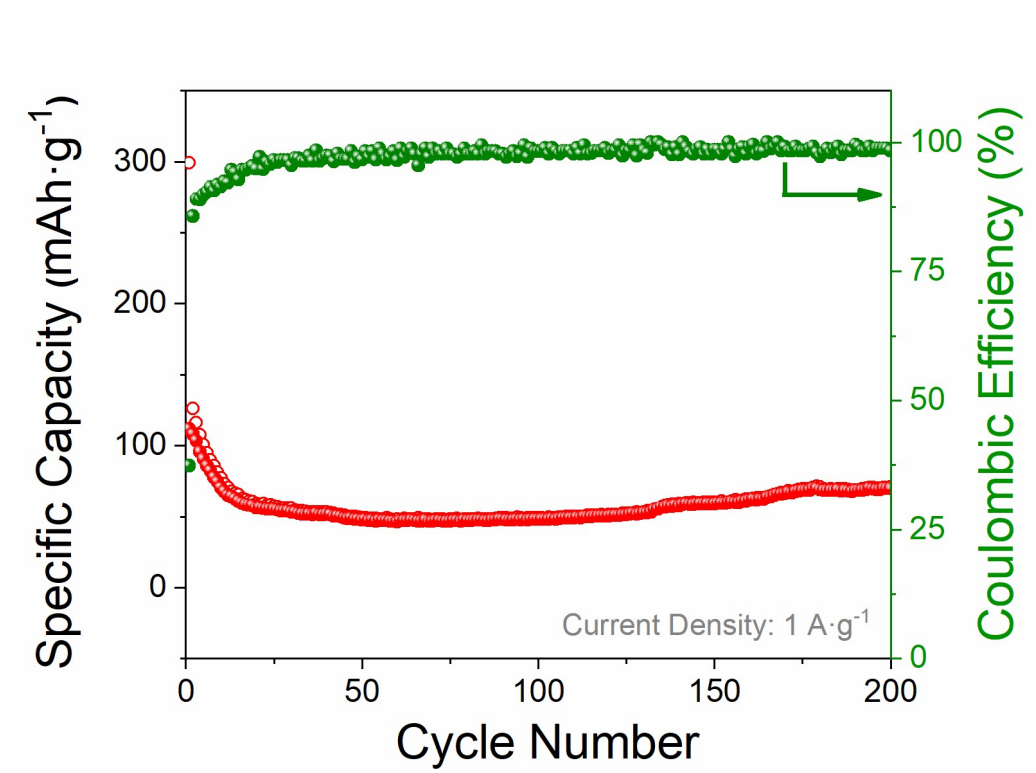

Fig. S9 SnS_2/Co_3S_4@CC//$Na_3V_2(PO_4)_2O_2F$ constant current cycle performance of full cell battery at 1 $A \cdot g^{-1}$.

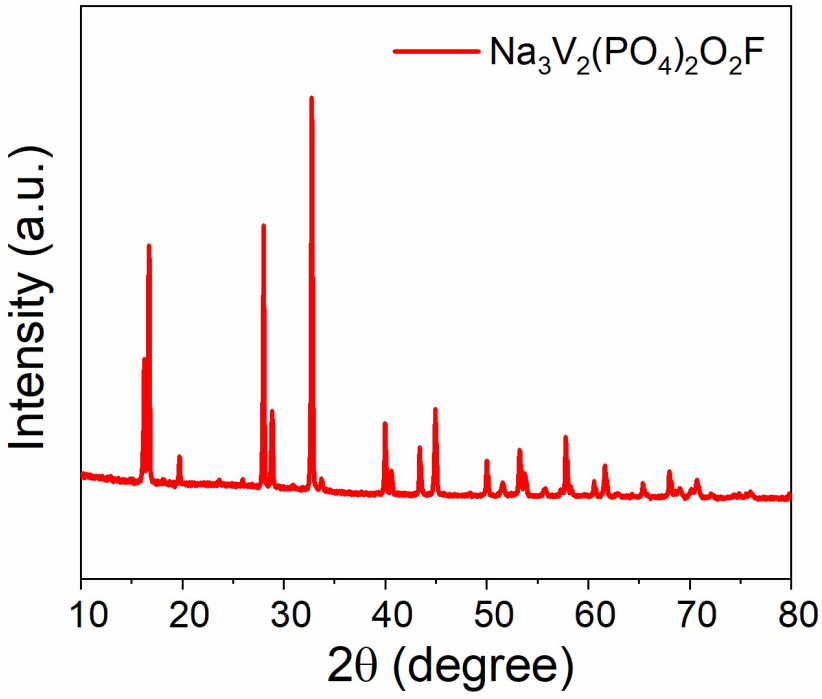

Fig. S10 XRD pattern of the $Na_3V_2(PO_4)_2O_2F$ material.

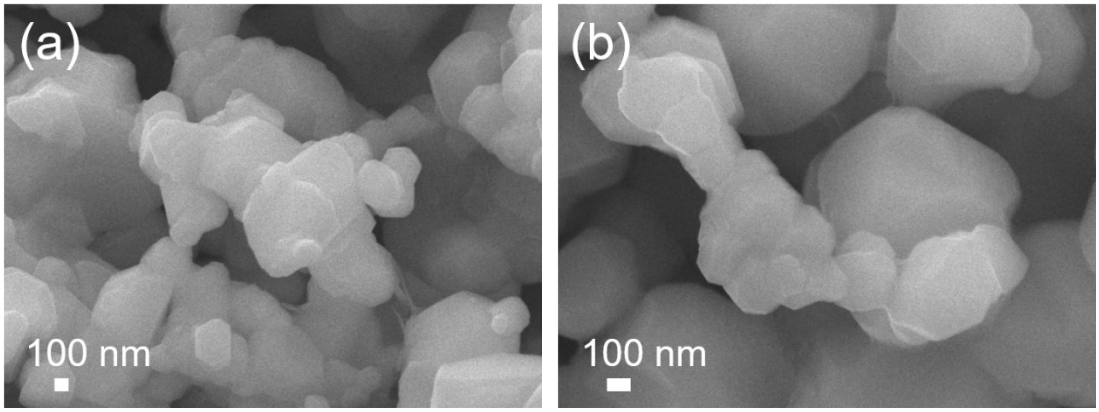

Fig. S11 (a, b) SEM images of the $Na_3V_2(PO_4)_2O_2F$ electrode.

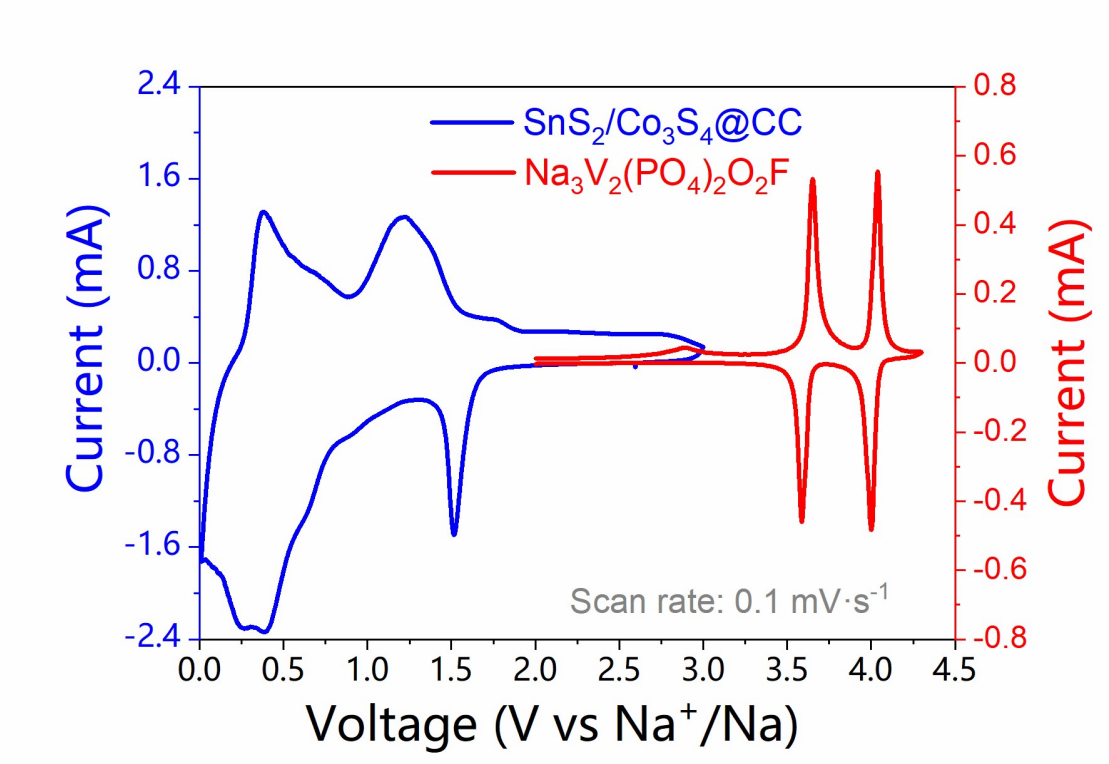

Fig. S12 CV curves of $Na_3V_2(PO_4)_2O_2F$ cathode and SnS_2/Co_3S_4@CC anode in half cells.

Table S2. R_2, σ and D_{Na+} values for the SnS_2@CC and SnS_2/Co_3S_4@CC electrodes

	R_2 (Ω)	σ (Ω $cm^2s^{-0.5}$)	D_{Li+}(cm^2s^{-1})
SnS_2/Co_3S_4@CC	46.3	26.35	4.0728×10^{-14}
SnS_2@CC	97.2	72.25	5.5049×10^{-15}

Table S3. ICP test and analysis data of the SnS_2/Co_3S_4@CC

SnS_2/Co_3S_4@CC (mg)	Co (mg/L)	Co (wt %)	Co_3S_4 (wt %)
	0.85	0.93	1.60
90.70	Sn (mg/L)	Sn (wt %)	SnS_2 (wt %)
	5.67	6.26	9.64

Table S4. ICP test and analysis data of the SnS_2@CC

SnS_2@CC (mg)	Sn (mg/L)	Sn (wt %)	SnS_2 (wt %)
73.40	4.58	6.24	9.61

References

1. D. Chao, C. Zhu, P. Yang, X. Xia, J. Liu, J. Wang, X. Fan, S. Savilov, J. Lin, H. Fan and Z. Shen, *Nat. Commun.*, 2016, **7**, 12122.
2. C. Ma, J. Xu, J. Alvarado, B. Qu, J. Somerville, J. Lee and Y. Meng, *Chem. Mater.*, 2015, **27**, 5633-5640.
3. P. Dutta, U. Sen and S. Mitra, *RSC Adv.*, 2014, **4**, 43155-43159.
4. Y. Zheng, T. Zhou, C. Zhang, J. Mao, H. Liu and Z. Guo, *Angew. Chem. Int. Ed.*, 2016, **55**, 3408-3413.
5. X. Xie, D. Su, S. Chen, J. Zhang, S. Dou and G. Wang, *Chem Asian J*, 2014, **9**, 1611-1617.
6. Y. Jiang, Y. Feng, B. Xi, S. Kai, K. Mi, J. Feng, J. Zhang and S. Xiong, *J. Mater. Chem. A*, 2016, **4**, 10719-10726.
7. B. Qu, C. Ma, G. Ji, C. Xu, J. Xu, Y. Meng, T. Wang and J. Lee, *Adv. Mater.*, 2014, **26**, 3854-3859.
8. L. Wang, J. Yuan, Q. Zhao, Z. Wang, Y. Zhu, X. Ma and C. Cao, *Electrochim. Acta*, 2019, **308**, 174-184.
9. Y. Wu, H. Yang, Y. Yang, H. Pu, W. Meng, R. Gao and D. Zhao, *Small*, 2019, **15**, 1903873.
10. L. Cao, B. Zhang, X. Ou, C. Wang, C. Peng and J. Zhang, *Small*, 2019, **15**, 1804861.